Journal of Science and Technology in Civil Engineering NUCE 2020. 14 (1): 1–14

A HYBRID ANALYTICAL-NUMERICAL SOLUTION FOR A CIRCULAR PILE UNDER LATERAL LOAD IN MULTILAYERED SOIL

Nghiem Manh Hien[a,*]

[a]*College of Information Technology and Engineering, Marshall University, One John Marshall Drive, Huntington, WV 25755, USA*

Article history:
Received 17/12/2019, Revised 15/01/2020, Accepted 15/01/2020

Abstract

A hybrid analytical-numerical solution is proposed to solve the problem of a laterally loaded pile with a circular cross-section in multilayered soils. In the pile-soil model, the lateral load is located at the pile head including both lateral force and bending moment. The single pile is considered as a beam on elastic foundation while shear beams model the soil column below the pile toe. The differential equations governing pile deflections are derived based on the energy principles and variational approaches. The differential equations are solved iteratively by using the finite element method that provides results of pile deflection, rotation angle, shear force, and bending moment along the pile and equivalent stiffness of the pile-soil system. The modulus reduction equation is also developed to match the proposed results well to the three-dimensional finite element analyses. Several examples are conducted to validate the proposed method by comparing the analysis results with those of existing analytical solutions, the three-dimensional finite element solutions.

Keywords: beam on elastic foundation; finite element method; pile; energy principle; lateral load.

https://doi.org/10.31814/stce.nuce2020-14(1)-01 © 2020 National University of Civil Engineering

1. Introduction

Pile foundations support super-structures like high-rise buildings, bridge abutments, and piers, earth-retaining structures, offshore structures. Horizontal forces caused by lateral loads such as wind, wave, traffic and seismic applying on the structures transmit to the piles in terms of lateral forces and bending moments located at the pile head. The piles subjected to lateral forces and bending moments at the pile head are analyzed in practice using beam on elastic foundation method, the three-dimensional (3D) finite element method, and finite difference method. In the beam on elastic foundation method, the pile is divided into small segments, and the surrounding soil is modeled by a series of independent springs [1–5]. In this approach, no interaction between these springs is considered, called the one-parameter approach [6]. Pasternak [7] and Georgiadis and Butterfield [8] proposed a spring model to improve the shortcoming of the one-parameter approach by considering shear interaction between these springs, called the two-parameter approach [9]. The pile deflection is determined by solving a four-order differential equation by using the method of initial parameter [9–11] (MIP). Recently, a continuum-based approach is developed [6, 12–14] based on the energy

*Corresponding author. *E-mail address:* hiennghiem@ssisoft.com (Hien, N. M.)

principles and variational approach initially proposed by Sun [15]. In this approach, the soil displacement is approximated by a product of the pile displacement and a dimensionless function representing the variation of the soil displacement in the radial direction. Basu and Salgado [6] modify the existing MIP to account for changes in soil properties due to soil layering and obtain analytical solutions.

The finite element method [16–19], finite elements coupled with Fourier series [20], the finite difference method [21], and the boundary element method [22] have been applied to analyze laterally loaded piles. If the finite element or finite difference methods are used, the number of discretized pile elements will have to be very large, resulting in increased computation time. Higgins [23] conducted laterally loaded pile analyses using the Fourier finite-element (FE) code developed by Smith and Griffiths [24]. The model is represented by a two-dimensional (2D) rectangular plane, which calculates the response of axisymmetric solids subject to non-axisymmetric loads. Three-dimensional finite element and finite difference methods are more accurate since it covers all effects without any major assumption but they are not appropriate for design purpose because of the time-consuming process.

Simplicity and acceptable accuracy are keys of any solution method among practicing engineers. The existing methods presented so far in predicting pile behavior under lateral load still experience difficulties in practice because of solution complexity and time-consuming process. The author proposed a simple and efficient solution in analyzing the performance of a single pile with circular cross-section under lateral load in multilayered soils based on the iterative solution scheme initially developed by Nghiem [19] and Nghiem and Chang [25, 26]. The differential equations are developed based on the method proposed by Sun [15] and solved by the finite element method.

2. Pile-soil model

A circular pile of length L_p and Young's modulus E_p with circular cross-section of radius r_p shows in Figs. 1a and 1b. The pile is under axial load P applied at the center of the cross-section and embedded in multi-layered soil medium with a total of n horizontal soil layers. The pile penetrates through m soil layers, and the pile toe is assumed to locate at the bottom of the m^{th} layer then underlain by $n - m$ soil layers. Properties of the i^{th} soil layer include Young's modulus, E_i Poisson's ratio ν_i, shear modulus, G_i and thickness H_i. The pile and soil column (below the pile toe) are modeled by M beam and (N-M) bar elements, respectively, as shown in Fig. 1. If soil modulus varies with depth

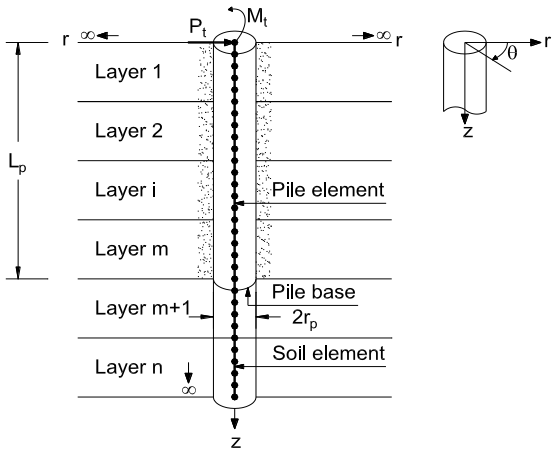
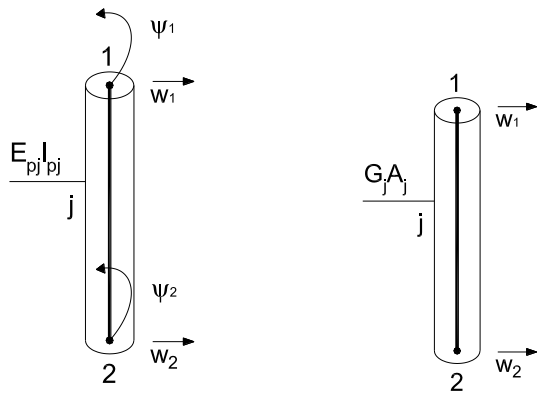


Figure 1. Pile-soil geometry



(a) Pile element (b) Soil element

Figure 2. The finite elements

in each layer, the pile and soil segments are divided into several sub-elements, and the modulus is approximated as a constant in each sub-element. The i^{th} soil layer surrounds the j^{th} pile element of length L_j (Fig. 2). The model uses a cylindrical coordinate system with its origin located at the center of the pile cross-section at the pile head and positive z-axis pointing downward, coinciding with the pile axis. The pile and soil elements and soil properties are assumed to be isotropic, homogeneous, and linear elastic, and the displacements at pile-soil interface compatible.

3. Displacement-strain-stress relationships

The assumption of the displacement field is proposed by Sun [15] for a pile under lateral load. Strains in the vertical direction are very small compared to the strains in the horizontal direction and can be assumed negligible. Since the lateral displacement in radial direction decreases with increases in radial distance from the pile, the lateral displacement field in the soil can be approximated by a product of separable variables as [6, 15]:

$$u_r(r,z) = w\phi\cos\theta \tag{1a}$$

$$u_\theta(r,z) = -w\phi\sin\theta \tag{1b}$$

where w is the lateral displacement of the pile at a depth of z; ϕ is the dimensionless function describing the reduction of the displacement in radial direction from the pile center. It is assumed that $\phi = 1$ at $r = r_p$ and $\phi = 0$ at $r = \infty$.

With the above assumptions, the strain-displacement relationship is given by:

$$\begin{Bmatrix} \varepsilon_r \\ \varepsilon_\theta \\ \varepsilon_z \\ \gamma_{r\theta} \\ \gamma_{rz} \\ \gamma_{z\theta} \end{Bmatrix} = \begin{Bmatrix} -\dfrac{\partial u_r}{\partial r} \\ -\dfrac{u_r}{r} - \dfrac{1}{r}\dfrac{\partial u_\theta}{\partial \theta} \\ -\dfrac{\partial u_z}{\partial z} \\ -\dfrac{1}{r}\dfrac{\partial u_r}{\partial \theta} - \dfrac{\partial u_\theta}{\partial r} + \dfrac{u_\theta}{r} \\ -\dfrac{\partial u_z}{\partial r} - \dfrac{\partial u_r}{\partial z} \\ -\dfrac{1}{r}\dfrac{\partial u_z}{\partial \theta} - \dfrac{\partial u_\theta}{\partial z} \end{Bmatrix} = \begin{Bmatrix} -w\dfrac{d\phi}{dr}\cos\theta \\ 0 \\ 0 \\ w\left(\dfrac{d\phi}{dr}\right)\sin\theta \\ -\dfrac{dw}{dz}\phi\cos\theta \\ \dfrac{dw}{dz}\phi\sin\theta \end{Bmatrix} \tag{2}$$

The relationships between stress and strain in soil can be written in general form based on Hooke's law as follows:

$$\begin{Bmatrix} \sigma_r \\ \sigma_\theta \\ \sigma_z \\ \tau_{r\theta} \\ \tau_{rz} \\ \tau_{z\theta} \end{Bmatrix} = \begin{bmatrix} \lambda+2G & \lambda & \lambda & 0 & 0 & 0 \\ \lambda & \lambda+2G & \lambda & 0 & 0 & 0 \\ \lambda & \lambda & \lambda+2G & 0 & 0 & 0 \\ 0 & 0 & 0 & G & 0 & 0 \\ 0 & 0 & 0 & 0 & G & 0 \\ 0 & 0 & 0 & 0 & 0 & G \end{bmatrix} \begin{Bmatrix} \varepsilon_r \\ \varepsilon_\theta \\ \varepsilon_z \\ \gamma_{r\theta} \\ \gamma_{rz} \\ \gamma_{z\theta} \end{Bmatrix} \tag{3}$$

where G and λ are Lamé's constants of soil.

4. Governing equilibrium equations

Potential energy Π of the soil-pile system defined as the sum of internal energy and external energy can be expressed by [6, 15]:

$$\Pi = \sum_{j=1}^{M} \frac{1}{2} \int_0^{L_j} E_{pj} I_{pj} \left(\frac{d^2 w_j}{dz^2} \right)^2 dz + \frac{1}{2} \sum_{j=M+1}^{N} \int_0^{L_j} G_i A \left(\frac{dw_j}{dz} \right)^2 dz + \sum_{j=1}^{N} \frac{1}{2} \int_0^{L_j} \int_0^{2\pi} \int_{r_p}^{\infty} \sigma_{mn} \varepsilon_{mn} r dr d\theta dz - F_t w_t + M_t \psi_t \quad (4)$$

where E_{pj} is Young's modulus of the j^{th} pile element; I_{pj} is moment of inertia of the j^{th} pile cross-section; G_j is shear modulus of the i^{th} soil layer; A is area of the pile cross-section; w_j is displacement of the j^{th} element; F_t and M_t are lateral load and bending moment, respectively, applied on the pile head at the depth $z = z_0$; w_t and ψ_t are displacement and rotation angle, respectively, of the pile at the depth $z = z_0$.

Strain energy obtained by:

$$\frac{1}{2} \sigma_{mn} \varepsilon_{mn} = \frac{1}{2} (\lambda + 2G) \left(w \frac{d\phi}{dr} \cos\theta \right)^2 + \frac{1}{2} G \left[w \left(\frac{d\phi}{dr} \right) \sin\theta \right]^2 + \frac{1}{2} G \left(\frac{dw}{dz} \phi \right)^2 \quad (5)$$

where σ_{mn} and ε_{mn} are the stress and the strain tensors.

$$\begin{aligned} \Pi = & \sum_{j=1}^{M} \frac{1}{2} \int_0^{L_j} E_{pj} I_{pj} \left(\frac{d^2 w_j}{dz^2} \right)^2 dz + \frac{1}{2} \sum_{j=M+1}^{N} \int_0^{L_j} G_i A \left(\frac{dw_j}{dz} \right)^2 dz + \frac{1}{2} \pi \sum_{j=1}^{N} \int_0^{L_j} \int_{r_p}^{\infty} (\lambda_i + 3G_i) \left(w_j \frac{d\phi}{dr} \right)^2 r dr dz \\ & + \pi \sum_{j=1}^{N} \int_0^{L_j} \int_{r_p}^{\infty} G_i \left(\frac{dw_j}{dz} \phi \right)^2 r dr dz - F_t w_t + M_t \psi_t \end{aligned} \quad (6)$$

Minimizing the potential energy of the soil-pile system by equaling the first variation of the potential energy to zero, yields:

For the pile element:

$$\delta\Pi = A_1 \left(\psi_j \right) \delta\psi_j + B(\phi) \delta\phi = 0 \quad (7a)$$

For the soil element:

$$\delta\Pi = A_2 \left(\psi_j \right) \delta\psi_j + B(\phi) \delta\phi = 0 \quad (7b)$$

where:

$$A_1 \left(\psi_j \right) = \frac{\partial \Pi}{\partial w_j} = E_p I_p \frac{d^4 w_j}{dz^4} - 2\pi \int_{r_p}^{\infty} G_i (\phi)^2 r dr \frac{d^2 w_j}{dz^2} + \pi \int_{r_p}^{\infty} (\lambda_i + 3G_i) \left(\frac{d\phi}{dr} \right)^2 r dr w_j \quad (8a)$$

$$A_2 \left(\psi_j \right) = \frac{\partial \Pi}{\partial w_j} = -G_i A \frac{d^2 w_j}{dz^2} - 2\pi \int_{r_p}^{\infty} G_i (\phi)^2 r dr \frac{d^2 w_j}{dz^2} + \pi \int_{r_p}^{\infty} (\lambda_i + 3G_i) \left(\frac{d\phi}{dr} \right)^2 r dr w_j \quad (8b)$$

$$B(\phi) = \frac{\partial \Pi}{\partial \phi} = -\pi \sum_{j=1}^{N} \int_0^{L_j} (\lambda_i + 3G_i) \left(w_j \right)^2 dz \frac{d^2 \phi}{dr^2} r - \pi \sum_{j=1}^{N} \int_0^{L_j} (\lambda_i + 3G_i) \left(w_j \right)^2 dz \frac{d\phi}{dr} + 2\pi \sum_{j=1}^{N} \int_0^{L_j} G_i \left(\frac{dw_j}{dz} \right)^2 dz \phi r \quad (9)$$

Because the functions $A_1\left(\psi_j\right)$, $A_2\left(\psi_j\right)$ and $B\left(\phi\right)$ are unknown while $\delta\psi_j$ and $\delta\phi$ are not zero, solutions for Eq. (7) can be obtained by assigning $A_1\left(\psi_j\right)$, $A_2\left(\psi_j\right)$ and $B\left(\phi\right)$ equal to zero. The following differential equations for the elements are obtained from $A_1\left(\psi_j\right) = 0$, and $A_2\left(\psi_j\right) = 0$:

$$E_p I_p \frac{d^4 w_j}{dz^4} - \left(2\pi \int_{r_p}^{\infty} G_i \phi^2 r dr\right) \frac{d^2 w_j}{dz^2} + \left[\pi \int_{r_p}^{\infty} (\lambda_i + 3G_i) \left(\frac{d\phi}{dr}\right)^2 r dr\right] w_j = 0 \tag{10a}$$

$$\left(G_i A + 2\pi \int_{r_p}^{\infty} G_i \phi^2 r dr\right) \frac{d^2 w_j}{dz^2} - \left[2\pi G_i \int_{r_p}^{\infty} \left(\frac{d\phi}{dr}\right)^2 r dr\right] w_j = 0 \tag{10b}$$

Eq. (10) can be written in short form as:

$$E_{pj} I_{pj} \frac{d^4 w_j}{dz^4} - h_j \frac{d^2 w_j}{dz^2} + k_j w_j = 0 \tag{11a}$$

$$\left(G_i A + t_j\right) \frac{d^2 w_j}{dz^2} - k_j w_j = 0 \tag{11b}$$

where k_j, h_j and t_j are subgrade reactions for shearing and axial resistances, respectively, and determined by:

$$h_j = 2\pi G_i \int_{r_p}^{\infty} \phi^2 r dr \tag{12a}$$

$$k_j = \pi \int_{r_p}^{\infty} (\lambda_i + 3G_i) \left(\frac{d\phi}{dr}\right)^2 r dr \tag{12b}$$

$$t_j = 2\pi \bar{E}_i \int_{r_p}^{\infty} \phi^2 r dr \tag{12c}$$

According to the finite element method, lateral displacement in a bar element is approximated by nodal displacements as (Fig. 1):

For the pile element:

$$w_j = N_1 w_{j,1} + N_2 \psi_{j,1} + N_3 w_{j,2} + N_4 \psi_{j,2} \tag{13}$$

For the soil element:

$$w_j = N_5 w_{j,1} + N_6 w_{j,2} \tag{14}$$

where $w_{j,1}$ and $w_{j,2}$ are lateral displacements at the first node and the second node of j^{th} element, respectively; $\psi_{j,1}$ and $\psi_{j,2}$ are rotation angles at the first node and the second node of j^{th} pile element, respectively, $\psi_{j,1} = dw_j/dz$ at the first node and $\psi_{j,2} = dw_j/dz$ at the second node; N_1 to N_6 are shape functions. The shape functions can be obtained by using the following functions [24]:

$$N_1 = \frac{1}{L_j^3}\left(L_j^3 - 3L_j z^2 + 2z^3\right); \quad N_2 = \frac{1}{L_j^2}\left(L_j^2 z - 2L_j z^2 + z^3\right); \quad N_3 = \frac{1}{L_j^3}\left(3L_j z^2 - 2z^3\right); \tag{15a}$$

$$N_4 = \frac{1}{L_j^2}\left(-L_j z^2 + z^3\right); \quad N_5 = 1 - \frac{z}{L_j}; \quad N_6 = \frac{z}{L_j} \tag{15b}$$

Substituting Eq. (15) into Eq. (11) gives the following equations:

$$\begin{aligned} E_{pj}I_{pj}\frac{d^4}{dz^4}\begin{bmatrix} N_1 & N_2 & N_3 & N_4 \end{bmatrix}\begin{Bmatrix} w_{1,j} \\ \psi_{1,j} \\ w_{2,j} \\ \psi_{2,j} \end{Bmatrix} - h_j\frac{d^2}{dz^2}\begin{bmatrix} N_1 & N_2 & N_3 & N_4 \end{bmatrix}\begin{Bmatrix} w_{1,j} \\ \psi_{1,j} \\ w_{2,j} \\ \psi_{2,j} \end{Bmatrix} \\ + k_j\begin{bmatrix} N_1 & N_2 & N_3 & N_4 \end{bmatrix}\begin{Bmatrix} w_{1,j} \\ \psi_{1,j} \\ w_{2,j} \\ \psi_{2,j} \end{Bmatrix} = 0 \end{aligned} \tag{16a}$$

$$s_j\frac{d^2}{dz^2}\begin{bmatrix} N_5 & N_6 \end{bmatrix}\begin{Bmatrix} w_{j,1} \\ w_{j,2} \end{Bmatrix} - k_j\begin{bmatrix} N_5 & N_6 \end{bmatrix}\begin{Bmatrix} w_{j,1} \\ w_{j,2} \end{Bmatrix} = 0 \tag{16b}$$

where $s_j = G_i A + t_j$.

Integrating Eq. (16) by Galerkin method and Green theory [24] will lead to stiffness matrices of pile and soil spring as presented in Appendix A.

5. Solution of differential equations

By assigning $B(\phi) = 0$ in Eq. (9), the governing differential equation for the soil surrounding the pile and soil elements is given by:

$$\frac{d^2\phi}{dr^2} + \frac{1}{r}\frac{d\phi}{dr} - \kappa^2\phi = 0 \tag{17}$$

where:

$$\kappa^2 = \frac{2\sum_{j=1}^{N}\int_0^{L_j} G_i\left(\frac{dw_j}{dz}\right)^2 dz}{\sum_{j=1}^{N}\int_0^{L_j}(\lambda_i + 3G_i)\left(w_j\right)^2 dz} \tag{18}$$

Using displacement approximation in Eq. (14), Eq. (19) leads to:

$$\kappa^2 = \frac{2\sum_{j=1}^{N} G_i\left\{w_j\right\}^T [m_2]\left\{w_j\right\}}{\sum_{j=1}^{N}(\lambda_i + 3G_i)\left\{w_j\right\}^T [m_1]\left\{w_j\right\}} \tag{19}$$

where m_1 and m_2 are matrices (see in the Appendix A).

The differential Eq. (17) is a form of the modified Bessel differential equation and its solution is given by:

$$\phi = c_1 I_0(\kappa r) + c_2 K_0(\kappa r) \tag{20}$$

where I_0 is a modified zero-order Bessel function of the first kind, and K_0 is a modified zero-order Bessel function of the second kind. Apply the boundary conditions $\phi = 1$ at $r = r_p$, and $\phi = 0$ at $r = \infty$ to Eq. (20), solution of Eq. (17) leads to:

$$\phi = \frac{K_0(\kappa r)}{K_0(\kappa r_p)} \tag{21}$$

By introducing Eq. (21) into Eqs. (12a), (12b) and (12c), the subgrade reaction moduli can be obtained as:

$$h_j = 2\pi \int_{r_p}^{\infty} G_i \phi^2 r dr = \frac{\pi G_i r_p^2}{K_0^2(\kappa r_p)} \left[K_1^2(\kappa r_p) - K_0^2(\kappa r_p) \right] \tag{22a}$$

$$k_j = \pi \int_{r_p}^{\infty} (\lambda_i + 3G_i) \left(\frac{d\phi}{dr} \right)^2 r dr = \frac{\pi (\lambda_i + 3G_i) r_p^2 \kappa^2}{2K_0^2(\kappa r_p)} \left[K_0(\kappa r_p) K_2(\kappa r_p) - K_1^2(\kappa r_p) \right] \tag{22b}$$

$$t_j = 2\pi \int_{r_p}^{\infty} \bar{E}_i \phi^2 r dr = \frac{\pi \bar{E}_i r_p^2}{K_0^2(\kappa r_p)} \left[K_1^2(\kappa r_p) - K_0^2(\kappa r_p) \right] \tag{22c}$$

6. Equivalent stiffness

The equivalent stiffness of the soil-pile system is the ratio of the applied load and displacement at the pile head. Consider a finite element model of the pile-soil system in Fig. 3, where a spring represented by equivalent stiffness can model an element. The equivalent stiffness of the below element becomes the base stiffness of the above element. The following procedure is used to determine the equivalent of the pile and soil elements and also the pile-soil system.

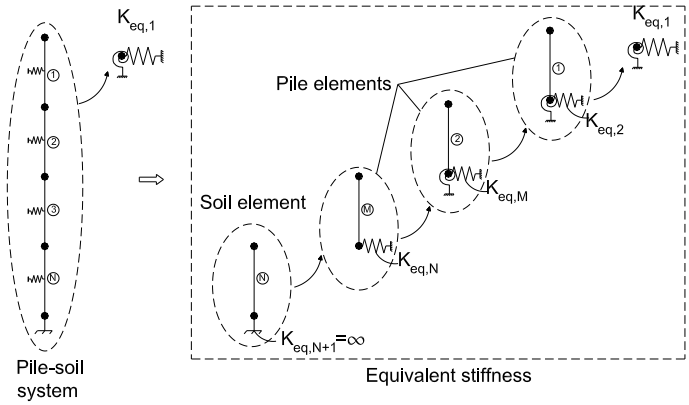


Figure 3. Equivalent stiffness of the pile-soil system

Stiffness matrix of the pile element is given in general form as follows:

$$\left[K_p\right]_j = \begin{bmatrix} k_{11} & k_{12} & k_{13} & k_{14} \\ & k_{22} & k_{23} & k_{24} \\ & sym. & k_{33} & k_{34} \\ & & & k_{44} \end{bmatrix} \tag{23}$$

Solving the following equations gives stiffness components of the equivalent stiffness matrix of the pile element in Eq. (24) as:

$$\begin{bmatrix} k_{11} & k_{13} & k_{14} \\ & k_{33} & k_{34} \\ sym. & & k_{44} \end{bmatrix} \begin{Bmatrix} w_1 \\ w_2 \\ \psi_2 \end{Bmatrix} = \begin{Bmatrix} 1 \\ 0 \\ 0 \end{Bmatrix}; \quad K_{11,j} = \frac{1}{w_1}; \quad K_{12,j} = \frac{k_{12}w_1 + k_{23}w_2 + k_{24}\psi_2}{w_1} \tag{24}$$

$$\begin{bmatrix} k_{22} & k_{23} & k_{24} \\ & k_{33} & k_{34} \\ sym. & & k_{44} \end{bmatrix} \begin{Bmatrix} \psi_1 \\ w_2 \\ \psi_2 \end{Bmatrix} = \begin{Bmatrix} 1 \\ 0 \\ 0 \end{Bmatrix}; \quad K_{22,j} = \frac{1}{\psi_1}; \quad K_{21,j} = \frac{k_{12}\psi_1 + k_{13}w_2 + k_{14}\psi_2}{\psi_1} \tag{25}$$

where:

$$K_{11,j} = \frac{k_{14}^2 k_{33} - 2k_{13}k_{14}k_{34} + k_{11}k_{34}^2 + k_{13}^2 k_{44} - k_{11}k_{33}k_{44}}{k_{34}^2 - k_{33}k_{44}} \tag{26a}$$

$$K_{22,j} = \frac{k_{24}^2 k_{33} - 2k_{23}k_{24}k_{34} + k_{22}k_{34}^2 + k_{23}^2 k_{44} - k_{22}k_{33}k_{44}}{k_{34}^2 - k_{33}k_{44}} \tag{26b}$$

$$K_{12,j} = K_{21,j} = \frac{-k_{14}k_{23}k_{34} + k_{12}k_{34}^2 + k_{14}k_{24}k_{33} - k_{13}k_{24}k_{34} - k_{12}k_{33}k_{44} + k_{13}k_{23}k_{44}}{k_{34}^2 - k_{33}k_{44}} \tag{26c}$$

Equivalent stiffness matrix of the j^{th} pile element is obtained in the following matrix form:

$$\left[K_{eq}\right]_j = \begin{bmatrix} K_{11,j} & K_{12,j} \\ K_{21,j} & K_{22,j} \end{bmatrix} \tag{27}$$

To determine the equivalent stiffness for the j^{th} soil element, the following equilibrium equation is formulated:

$$\left(\frac{s_j}{L_j} \begin{bmatrix} 1 & -1 \\ -1 & 1 \end{bmatrix} + k_j L_j \begin{bmatrix} \frac{1}{3} & \frac{1}{6} \\ \frac{1}{6} & \frac{1}{3} \end{bmatrix} + \begin{bmatrix} 0 & 0 \\ 0 & K_{eq,j+1} \end{bmatrix} \right) \begin{Bmatrix} w_1 \\ w_2 \end{Bmatrix} = \begin{Bmatrix} 1 \\ 0 \end{Bmatrix} \tag{28}$$

The equivalent stiffness of the j^{th} soil element is then calculated as $K_{eq,j} = 1/w_1$ or:

$$K_{eq,j} = \frac{\left(12s_j + 4k_j L_j^2\right) K_{eq,j+1} + 12s_j k_j L_j + k_j^2 L_j^3}{4\left(3s_j + 3K_{eq,j+1}L_j + k_j L_j^2\right)} \tag{29}$$

7. Iterative solution for the soil-pile system

The iterative solution for the pile-soil system is originally developed by Nghiem and Chang [25, 26] and extends to solve the problem of the pile under lateral load. The method is based on the equivalent stiffness approach as presented in section 6.

The solution scheme is given in the following steps:

Step 1: Assumption was made that initial values of lateral displacements and rotations, $w_j = 0$ and $\psi_j = 0$ for all elements.

Step 2: Calculate equivalent stiffness:

- Loop from element to element: $j = N \rightarrow 1$: At the base of the soil column: $K_{eq,N+1} = \infty$

+ Calculate stiffnesses of springs by using Eqs. (22a), (22b), and (22c)

+ Calculate equivalent stiffness of each element $K_{eq,j}$ from Eq. (29) if $j > M$, and Eq. (27) if $j \leq M$. The stiffnesses of soil springs in all elements are tangential and equivalent stiffness $K_{eq,1}$ of the 1st element is equal to the equivalent stiffness of the whole pile and soil system.

Step 3: Calculate the displacements and rotations:

- The displacement and rotation at the first end of the j^{th} element:

+ If $j = 1$ then:

$$\begin{bmatrix} K_{11,1} & K_{12,1} \\ K_{21,1} & K_{22,1} \end{bmatrix} \begin{Bmatrix} w_{1,1} \\ \psi_{1,1} \end{Bmatrix} = \begin{Bmatrix} F_t \\ M_t \end{Bmatrix} \tag{30}$$

Solving Eq. (30) gives the displacement and rotation angle as follows:

$$w_{1,1} = \frac{-K_{12,1}M_t + K_{22,1}F_t}{K_{11,1}K_{22,1} - K_{12,1}^2} \quad \text{and} \quad \psi_{1,1} = \frac{K_{11,1}M_t - K_{12,1}F_t}{K_{11,1}K_{22,1} - K_{12,1}^2} \tag{31}$$

+ If $1 < j \leq M$ then:

$$\begin{cases} w_{1,j} = w_{2,j-1} \\ \psi_{1,j} = \psi_{2,j-1} \end{cases} \tag{32}$$

+ If $j > M$ then:

$$w_{1,j} = w_{2,j-1} \tag{33}$$

- The displacements and rotations at the second end of the j^{th} element:

+ If $1 \leq j < M$ then the displacement and rotations at the second end are obtained by solving the following equations:

$$\begin{bmatrix} k_{33,j} + K_{11,j+1} & k_{34,j} + K_{12,j+1} \\ k_{43,j} + K_{21,j+1} & k_{44,j} + K_{22,j+1} \end{bmatrix} \begin{Bmatrix} w_{2,j} \\ \psi_{2,j} \end{Bmatrix} = \begin{Bmatrix} -k_{31}w_{1,j} - k_{32}\psi_{1,j} \\ -k_{41}w_{1,j} - k_{42}\psi_{1,j} \end{Bmatrix} \tag{34}$$

+ If $M < j \leq N$ then

$$w_{2,j} = \frac{K_{11,j}w_{1,j} - k_{11,j}w_{1,j}}{k_{12,j}} \tag{35}$$

- The forces at the first end of the j^{th} element:

+ If $j = 1$ then:

$$\begin{Bmatrix} F_{1,j} \\ M_{1,j} \end{Bmatrix} = \begin{bmatrix} K_{11,j} & K_{12,j} \\ K_{21,j} & K_{22,j} \end{bmatrix} \begin{Bmatrix} w_{1,j} \\ \psi_{1,j} \end{Bmatrix} \tag{36}$$

- The forces at the second end of the j^{th} element:

+ If $1 \leq j < M$ then

$$\begin{Bmatrix} F_{2,j} \\ M_{2,j} \end{Bmatrix} = \begin{bmatrix} k_{31,j} & k_{32,j} & k_{33,j} & k_{34,j} \\ k_{41,j} & k_{42,j} & k_{43,j} & k_{44,j} \end{bmatrix} \begin{Bmatrix} w_{1,j} \\ \psi_{1,j} \\ w_{2,j} \\ \psi_{2,j} \end{Bmatrix} \tag{37}$$

+ If $M \leq j \leq N$ then:

$$F_{2,j} = k_{12,j}w_{1,j} + k_{22,j}w_{2,j} \tag{38}$$

8. Modulus reduction

If Poisson's ratio, $\nu \rightarrow 0.5$ or $\lambda = \nu E/(1-2\nu)(1+\nu) \rightarrow \infty$, the subgrade reaction in the Eqs. (22b) and (22c) reaches an extremely large number and the pile response becomes increasingly stiffer. Guo and Lee [12] first observed this problem from unrealistic results of the solution proposed by Sun [15] for the Poisson's ratio greater than 0.3. Guo and Lee [12] further pointed out the equations $\bar{G} = 0.75(1+0.75\nu)G$ and $\bar{\lambda} = 0$ can be used to produce reliable results in comparison to those of the 3D finite element analyses. Basu and Salgado [6] verified the modulus reduction equations proposed by Guo and Lee [12] for the pile embedded in multi-layered soil media and the stiff pile response still observed. The stiff pile response arises from the fact that the assumed displacement field (Eq. (1)) produces zero displacement in the soil mass perpendicular to the direction of the applied force. To reduce the artificial stiffness, Basu and Salgado [6] reduce the shear modulus of the soil as shown in the following equation to match the finite element results closely:

$$G^* = 0.75(1+0.75\nu)G \quad \text{and} \quad \lambda^* = 0 \tag{39}$$

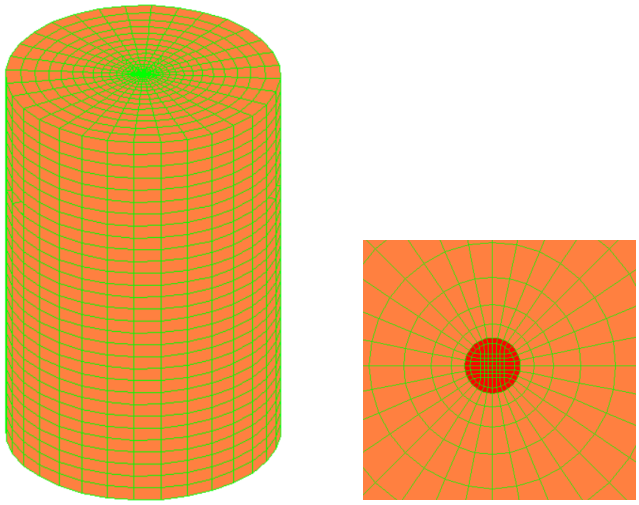
9. Comparison with previous and 3D finite element analyses

Consider a single pile with $r_p = 0.5$ m, $L_p = 20$ m, and $E_p = 27.5 \times 10^6$ kPa, embedded in a homogeneous soil with $E_s = 10000$ kPa, and Poisson's ratio varies from 0.001 to 0.499. The pile response also obtained from three sets of analyses using the proposed solution method. The first set of analyses is conducted without changing shear and constraint moduli. The second set of analyses are conducted that the moduli are reduced based on Eq. (39) proposed by Guo and Lee [12]. In the third set, new equations for modification of soil moduli are developed and applied in the analyses and given as follows:

$$G_s^* = 0.8\left[\frac{(1-2\nu)(1+\nu)}{1-\nu}\right]^{0.1}(1+0.75\nu)G_s \quad \text{and} \quad \lambda_s^* = 0 \tag{40}$$

3D finite element analyses using SSI3D program [19] are performed to verify the accuracy of the proposed solution method. Fig. 4 depicts the 3D finite element model where both pile and soil are modelled by 8-node hexagonal element. In the 3D finite element model, pile and soil are considered as linear elastic material and a free head pile is subjected to lateral load. The boundaries of the model are extended to a horizontal distance of $40r_p$ from center of the pile to avoid spurious reaction into the system. Soil only can move in the vertical direction at the vertical boundary and is fixed at the bottom boundary. Pile deflection has been used as benchmark for the proposed solution. Ratios between pile head displacements of the proposed solution and the 3D finite element solution are presented in Fig. 5. It is evident from Fig. 5 that the pile head deflection ratios obtained from the first set of analyses progressively deviate from the 3D finite element analysis results as the Poisson's ratio of soil increases from 0.3. With the Poisson's ratio less than 0.3, the proposed method produces the pile head deflection ratios approximately 80% of those predicted by the 3D finite element analyses. The better approximation of the pile head deflection obtained in the second set of analyses with differences from the 3D finite element analyses less than 10% for the Poisson's ratios lower than 0.4 while using the simple modification equations of the soil moduli (Eq. (39)) by Guo and Lee [12]. The results of the pile head deflection are not in good agreement for the Poisson's ratios greater than 0.4. To reduce differences of the pile head deflection shown in the above analyses, the third set of analyses are conducted using Eq. (40). As also shows in Fig. 3, the pile head deflections are in good match

with those from the 3D finite element analyses. Fig. 6 shows the pile deflection profiles obtained from the proposed method and the 3D finite element analyses with a very good match between the two methods.



(a) 3D view (b) Plane view

Figure 4. 3D finite element model

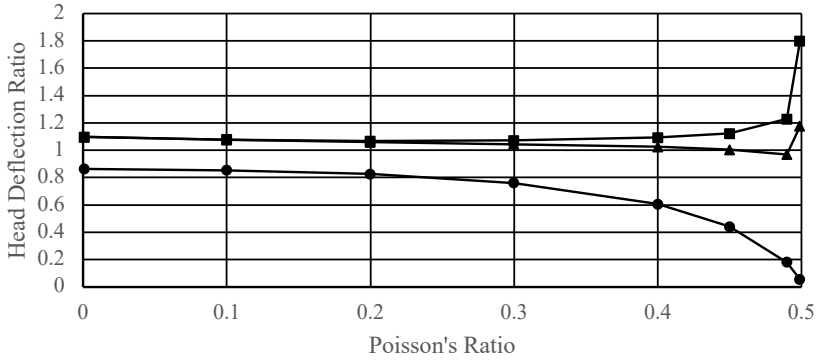


Figure 5. Pile head displacement ratios

A comparison of pile deflections between the proposed method and the 3D finite element method has been made to verify the accuracy of the proposed method for a pile under lateral load in nonhomogeneous soil. The circular pile with $r_p = 0.5$ m, $L_p = 15$ m, and $E_p = 24 \times 10^3$ MPa, embedded in four-layer soil media with Young's modulus of $E_{s1} = 20$ MPa, $E_{s2} = 35$ MPa, $E_{s3} = 50$ MPa, and $E_{s4} = 80$ MPa, Poisson's ratios of $\nu_{s1} = 0.35$, $\nu_{s2} = 0.25$, $\nu_{s3} = 0.2$, and $\nu_{s4} = 0.15$, and soil layer thicknesses of $H_1 = 2$ m, $H_2 = 5$ m, $H_3 = 8$ m. A force $P = 300$ kN is applied at the pile head. Fig. 7 shows the pile deflection for three cases of analyses: no modulus reduction, modulus reduction using Eq. (40), and the 3D finite element analysis. The pile deflections obtained from the proposed method with modulus reduction matches better than that from the proposed method without modulus reduction in comparison to the result obtained from the 3D finite element analysis.

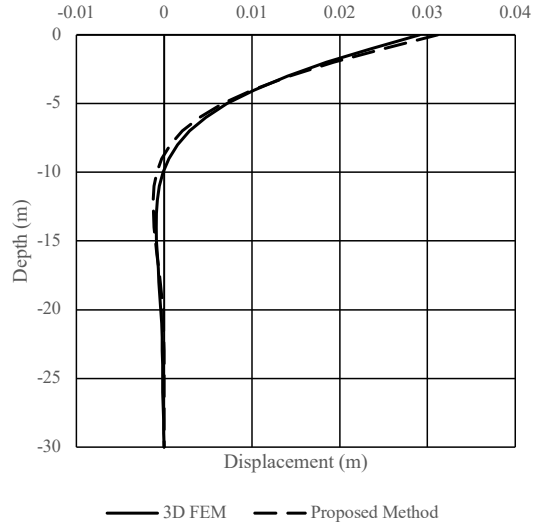


Figure 6. Pile deflection profile for 20 m long pile

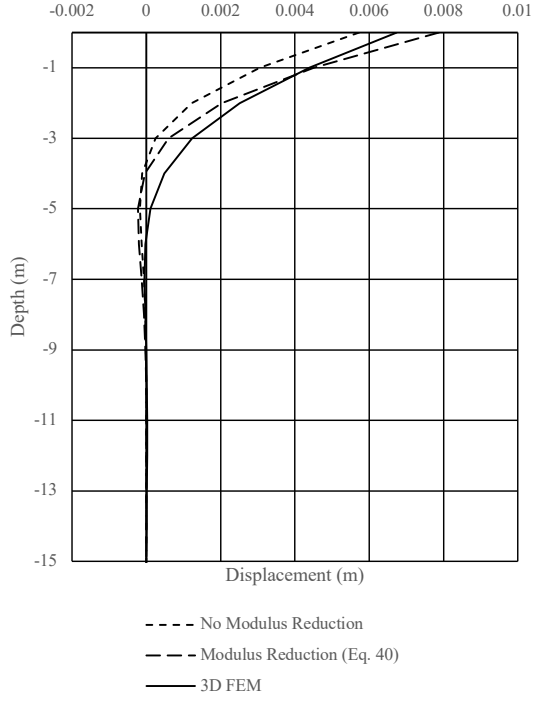


Figure 7. Pile deflection profile for 15 m long pile

10. Conclusion

This paper presents a simple, efficient and accurate method for performance analysis of a single pile embedded in multiple layers of different soils under a lateral load applied at the pile head. The governing equations were derived based on continuum mechanics, strain energy and variational calculus from the literature. A new equation for soil modulus reduction was developed by matching the displacement along the pile of the proposed method to those of the 3D finite element method.

The analysis results using the new solution scheme compared quite well with the results from another analytical method with the same theoretical basis studied by previous researchers and the 3D finite element analyses.

References

[1] Winkler, E. (1867). *Die Lehre von der Elasticitaet und Festigkeit*. Prag: Dominicus.

[2] Terzaghi, K. (1955). Evalution of conefficients of subgrade reaction. *Geotechnique*, 5(4):297–326.

[3] Scott, R. F. (1981). *Foundation analysis*. Prentice Hall: Englewood Cliffs, NJ.

[4] Madhav, M. R., Rao, N. S. V. K., Madhavan, K. (1971). Laterally loaded pile in elasto-plastic soil. *Soils and Foundations*, 11(2):1–15.

[5] Valsangkar, A. J., Kameswara Rao, N. S. V., Basudhar, P. K. (1973). Generalized solutions of axially and laterally loaded piles in elasto-plastic soil. *Soils and Foundations*, 13(4):1–14.

[6] Basu, D., Salgado, R. (2007). Elastic analysis of laterally loaded pile in multi-layered soil. *Geomechanics and Geoengineering*, 2(3):183–196.

[7] Pasternak, P. L. (1954). On a new method of analysis of an elastic foundation by means of two foundation constants. *Gosudarstvennoe Izdatelstvo Literaturi po Stroitelstvu i Arkhitekture, Moscow, USSR*. (in Russian).

[8] Georgiadis, M., Butterfield, R. (1982). Laterally loaded pile behavior. *Journal of the Geotechnical Engineering Division*, 108(1):155–165.

[9] Vlasov, V. Z. (1966). Beams, plates and shells on elastic foundation. *Israel Program for Scientific Translation*.

[10] Harr, M. E., Davidson, J. L., Ho, D., Pombo, L. E., Ramaswamy, S. V., Rosner, J. C. (1969). Euler beams on a two parameter foundation model. *Journal of Soil Mechanics & Foundations Div*.

[11] Rao, N. S. V., Das, Y. C., Anandakrishnan, M. (1971). Variational approach to beams on elastic foundations. *Journal of the Engineering Mechanics Division*, 97(2):271–294.

[12] Guo, W. D., Lee, F. H. (2001). Load transfer approach for laterally loaded piles. *International Journal for Numerical and Analytical Methods in Geomechanics*, 25(11):1101–1129.

[13] Basu, D., Salgado, R. (2007). Method of initial parameters for laterally loaded piles embedded in layered soils. *Geomechanics and Geoengineering*, 2(4):281–294.

[14] Basu, D., Salgado, R., Prezzi, M. (2009). A continuum-based model for analysis of laterally loaded piles in layered soils. *Geotechnique*, 59:127–140.

[15] Sun, K. (1994). Laterally loaded piles in elastic media. *Journal of Geotechnical Engineering*, 120(8): 1324–1344.

[16] Desai, C. S., Appel, G. C. (1976). 3-D analysis of laterally loaded structures. In *Proceedings of the 2nd International Conference on Numerical Methods in Geomechanics, Blacksburg*, 405–418.

[17] Bransby, M. F. (1999). Selection of p–y curves for the design of single laterally loaded piles. *International Journal for Numerical and Analytical Methods in Geomechanics*, 23(15):1909–1926.

[18] Chang, N. Y., Nghiem, H. M. (2007). Nonlinear spring functions for 3D seismic responses of structures on piles. *Deep Foundation Institute*.

[19] Nghiem, H. M. (2009). *Soil-pile-structure interaction effects of high-rise building under seismic shaking*. Doctoral Dissertation, University of Colorado Denver.

[20] Randolph, M. F. (1981). The response of flexible piles to lateral loading. *Geotechnique*, 31(2):247–259.

[21] Ng, C. W. W., Zhang, L. M. (2001). Three-dimensional analysis of performance of laterally loaded sleeved piles in sloping ground. *Journal of Geotechnical and Geoenvironmental Engineering*, 127(6):499–509.

[22] Budhu, M., Davies, T. G. (1988). Analysis of laterally loaded piles in soft clays. *Journal of Geotechnical Engineering*, 114(1):21–39.

[23] Higgins, W., Vasquez, C., Basu, D., Griffiths, D. V. (2012). Elastic solutions for laterally loaded piles. *Journal of Geotechnical and Geoenvironmental Engineering*, 139(7):1096–1103.

[24] Smith, I. M., Griffiths, D. V. (2004). *Programming the finite element method*. Fourth edition, John Wiley & Sons.

[25] Nghiem, H. M., Chang, N.-Y. (2019). Efficient solution for a single pile under torsion. *Soils and Foundations*, 59(1):13–26.
[26] Nghiem, H. M., Chang, N.-Y. (2019). Pile under torque in nonlinear soils and soil-pile interfaces. *Soils and Foundations*.

Appendix A.

$$[K_1] = \frac{2E_{pj}I_{pj}}{L_j^3}\begin{bmatrix} 6 & 3L & -6 & 3L \\ 3L & 2L^2 & -3L & L^2 \\ -6 & -3L & 6 & -3L \\ 3L & L^2 & -3L & 2L^2 \end{bmatrix} \tag{A.1}$$

$$[K_2] = \frac{k_j}{30L_j}\begin{bmatrix} 36 & 3L_j & -36 & 3L_j \\ 3L_j & 4L_j^2 & -3L_j & -L_j^2 \\ -36 & -3L_j & 36 & -3L_j \\ 3L_j & -L_j^2 & -3L_j & 4L_j^2 \end{bmatrix} \tag{A.2}$$

$$[K_3] = \frac{h_jL_j}{420}\begin{bmatrix} 156 & 22L & 54 & -13L \\ 22L & 4L^2 & 13L & -3L^2 \\ 54 & 13L & 156 & -22L \\ -13L & -3L^2 & -22L & 4L^2 \end{bmatrix} \tag{A.3}$$

$$[K_4] = \frac{s_j}{L_j}\begin{bmatrix} 1 & -1 \\ -1 & 1 \end{bmatrix} \tag{A.4}$$

$$[K_5] = k_jL_j\begin{bmatrix} \frac{1}{3} & \frac{1}{6} \\ \frac{1}{6} & \frac{1}{3} \end{bmatrix} \tag{A.5}$$

For the pile element:

$$[m_1] = \frac{L}{420}\begin{bmatrix} 156 & 22L & 54 & -13L \\ 22L & 4L^2 & 13L & -3L^2 \\ 54 & 13L & 156 & -22L \\ -13L & -3L^2 & -22L & 4L^2 \end{bmatrix} \tag{A.6}$$

$$[m_2] = \frac{1}{30L}\begin{bmatrix} 36 & 3L & -36 & 3L \\ 3L & 4L^2 & -3L & -L^2 \\ -36 & -3L & 36 & -3L \\ 3L & -L^2 & -3L & 4L^2 \end{bmatrix} \tag{A.7}$$

For the soil element:

$$[m_1] = \frac{L}{6}\begin{bmatrix} 2 & 1 \\ 1 & 2 \end{bmatrix} \tag{A.8}$$

$$[m_2] = \frac{1}{L}\begin{bmatrix} 1 & -1 \\ -1 & 1 \end{bmatrix} \tag{A.9}$$